eNeuro

New Research

Neuronal Excitability

Contribution of Resting Conductance, $GABA_A$-Receptor Mediated Miniature Synaptic Currents and Neurosteroid to Chloride Homeostasis in Central Neurons

Tushar D. Yelhekar, Michael Druzin, and Staffan Johansson

DOI:http://dx.doi.org/10.1523/ENEURO.0019-17.2017

Department of Integrative Medical Biology, Umeå University, Umeå, SE-901 87, Sweden

Abstract

Maintenance of a low intraneuronal Cl^- concentration, $[Cl^-]_i$, is critical for inhibition in the CNS. Here, the contribution of passive, conductive Cl^- flux to recovery of $[Cl^-]_i$ after a high load was analyzed in mature central neurons from rat. A novel method for quantifying the resting Cl^- conductance, important for $[Cl^-]_i$ recovery, was developed and the possible contribution of $GABA_A$ and glycine receptors and of ClC-2 channels to this conductance was analyzed. The hypothesis that spontaneous, action potential-independent release of GABA is important for $[Cl^-]_i$ recovery was tested. $[Cl^-]_i$ was examined by gramicidin-perforated patch recordings in medial preoptic neurons. Cells were loaded with Cl^- by combining GABA or glycine application with a depolarized voltage, and the time course of $[Cl^-]_i$ was followed by measurements of the Cl^- equilibrium potential, as obtained from the current recorded during voltage ramps combined with GABA or glycine application. The results show that passive Cl^- flux contributes significantly, in the same order of magnitude as does K^+-Cl^- cotransporter 2 (KCC2), to $[Cl^-]_i$ recovery and that Cl^- conductance accounts for $\sim$ 6% of the total resting conductance. A major fraction of this resting Cl^- conductance is picrotoxin (PTX)-sensitive and likely due to open $GABA_A$ receptors, but ClC-2 channels do not contribute. The results also show that when the decay of $GABA_A$ receptor-mediated miniature postsynaptic currents (minis) is slowed by the neurosteroid allopregnanolone, such minis may significantly quicken $[Cl^-]_i$ recovery, suggesting a possible steroid-regulated role for minis in the control of Cl^- homeostasis.

Key words: chloride homeostasis; $GABA_A$ receptor; KCC2; miniature postsynaptic current; neurosteroid; resting chloride conductance

Significance Statement

The Cl^- concentration in central neurons is critical to normal synaptic function and if not properly regulated may contribute to epilepsy, chronic pain, and other pathologies. Here, we introduce a novel method to quantify the resting Cl^- conductance of the neuronal membrane and show how this conductance contributes to the recovery of Cl^- concentration after a high Cl^- load. We also clarify that ion channels of the $GABA_A$ receptor type underlie a major fraction of the resting Cl^- conductance and show that an endogenous neurosteroid may quicken recovery of Cl^- concentration via effects of spontaneously released neurotransmitter on the $GABA_A$ receptors. The findings are important for understanding the neuronal Cl^- homeostasis, critical to normal brain function.

Introduction

The intraneuronal Cl^- concentration, $[Cl^-]_i$, is critical for synaptic communication. The inhibitory actions of GABA and glycine depend on a relatively low $[Cl^-]_i$. $[Cl^-]_i$ may, however, rise as a consequence of intense synaptic activity. When excitatory inputs depolarize the membrane, the driving force for inward Cl^- flux through channels opened by GABA or glycine increases and may impose a strong Cl^- load on the neuron. Cl^- flows into the cell also during shunting inhibition (Doyon et al., 2016b). In some cases, the raised $[Cl^-]_i$ changes the effect of GABA to excitatory (Khalilov et al., 2003; Astorga et al., 2015). Restoring $[Cl^-]_i$ after large perturbations may thus be expected crucial for normal inhibitory GABAergic synaptic function. The K^+-Cl^- cotransporter 2 (KCC2) is critical for the control of $[Cl^-]_i$ and likely contributes significantly to $[Cl^-]_i$ restoration (Doyon et al., 2016b). However, as a consequence of the negative resting potential maintained by neurons, passive Cl^- flux through Cl^- conducting membrane pathways may also contribute to the recovery of a low $[Cl^-]_i$. In the absence of Cl^- transporters, the Cl^- equilibrium potential (E_{Cl}) will settle at the membrane resting potential. The relative importance of KCC2 and passive, "conductive" flux is at present unknown.

Conductive $[Cl^-]_i$ recovery depends on the resting membrane Cl^- conductance (g_{Cl}). There is, however, no generally accepted view on the resting Cl^- permeability or g_{Cl} in central neurons. A low resting permeability has been suggested by Thompson et al. (1988), but a significant conductance has been described in other studies (Forsythe and Redman, 1988; Sacchi et al., 1999; Müller, 2000).

The molecular basis for resting g_{Cl} is also not well understood. It has been proposed that ClC-2 channels are general contributors to the resting g_{Cl} in neurons (Rinke, 2010; but see Stölting et al., 2014). However, the expression of ClC-2 is highly restricted to specific neuronal types (Smith et al., 1995) or neuronal compartments (Földy et al., 2010). Another contribution to resting g_{Cl} may be provided by $GABA_A$ receptors, which underlie a tonic conductance in some neurons (Semyanov et al., 2004; Belelli et al., 2009).

Received January 14, 2017; accepted March 12, 2017; First published March 17, 2017.

The authors declare no competing financial interests.

Author contributions: T.D.Y., M.D., and S.J. designed research; T.D.Y. and S.J. performed research; T.D.Y., M.D., and S.J. analyzed data; T.D.Y., M.D., and S.J. wrote the paper.

This work was supported by the Swedish Research Council (Grant 22292), by Gunvor och Josef Anérs Stiftelse, and by Umeå University Medical Faculty (Insamlingsstiftelsen, Karin och Harald Silvanders fond, and Leila och Bertil Ehrengrens fond).

Correspondence should be addressed to Staffan Johansson, Department of Integrative Medical Biology, Umeå University, SE-901 87 Umeå, Sweden, E-mail: staffan.o.johansson@umu.se.

DOI:http://dx.doi.org/10.1523/ENEURO.0019-17.2017

It seems possible that also the spontaneous GABA release that is seen as miniature postsynaptic potentials/currents (minis) contributes significantly to resting g_{Cl}. The functional role of such minis is not clear. Although they imply relatively small currents, we hypothesized that they may be important for conductive recovery of $[Cl^-]_i$ after perturbations, at least when prolonged by endogenous neurosteroids that target $GABA_A$ receptors and in some conditions also enhance GABA release (Haage and Johansson, 1999).

In the present work, we estimated the contribution of passive Cl^- flux to $[Cl^-]_i$ recovery, in preoptic neurons from rat. We also developed a novel method to estimate the relative g_{Cl} at rest and analyzed whether ClC-2 channels and $GABA_A$ receptors contribute to resting g_{Cl}. Finally, we tested the hypothesis that spontaneous GABA release is important for $[Cl^-]_i$ recovery. To improve the electrical recording conditions and to avoid possible $[Cl^-]_i$ redistribution between neuronal compartments, we used acutely isolated neurons from which neurites were largely removed, but which retain attached presynaptic nerve terminals that enable analysis of spontaneous GABA release (Haage et al., 1998). Cells were loaded with Cl^- by combining GABA or glycine application with a depolarized voltage and $[Cl^-]_i$ was obtained from measurements of E_{Cl} by gramicidin-perforated patch recordings with GABA or glycine application in combination with voltage ramps (Karlsson et al., 2011; Yelhekar et al., 2016).

Here, we show that passive Cl^- flux contributes significantly to $[Cl^-]_i$ recovery after a high load, and, using our novel method, we also show that Cl^- conductance accounts for ~6% of the total resting conductance. A major fraction of this resting Cl^- conductance is picrotoxin (PTX)-sensitive and thus likely due to $GABA_A$ receptors. Further, we show that when the decay of $GABA_A$ receptor-mediated minis is slowed by the neurosteroid allopregnanolone, such minis contribute significantly to $[Cl^-]_i$ recovery, thus suggesting a possible steroid-regulated role for minis in the control of Cl^- homeostasis.

Materials and Methods

Ethical approval

All animal procedures were performed in accordance with the regulations of the regional ethics committee for animal research (Umeå djurförsöksetiska nämnd, approval number A9-14).

Preparation of neurons

Acutely dissociated neurons were prepared from in total 148 young, male Sprague Dawley rats, 50-110 g, three to five weeks of age (Karlsson et al., 1997). The animals were housed with *ad libitum* access to food and water under a 12/12 h light/dark cycle. They were killed by decapitation without anesthetics, the brain removed, and 200- to 300-μm-thick coronal slices containing the medial preoptic area were cut. Individual neurons were isolated by application of a vibrating glass rod just above the slice, at the location of the medial preoptic nucleus. The major parts of neurites were thus removed, but functional pre-

synaptic terminals remained attached to the postsynaptic cell bodies (Haage et al., 1998).

Solutions used for preparation and for recording

A solution of the following composition was used to cut and incubate brain slices and for mechanical dissociation of individual neurons: 150 mM NaCl, 5.0 mM KCl, 2.0 mM $CaCl_2$, 1.2 mM $MgCl_2$, 10 mM HEPES, 10 mM glucose, and 4.93 mM Tris-base, pH 7.4 (95% O_2, 5% CO_2). The extracellular solution used for recording contained: 137 mM NaCl, 5.0 mM KCl, 1.0 mM $CaCl_2$, 1.2 mM $MgCl_2$, 10 mM HEPES, and 10 mM glucose, pH 7.4 (NaOH). The standard pipette-filling solution contained: 140 mM K-gluconate, 3.0 mM NaCl, 1.2 mM $MgCl_2$, 10 mM HEPES, and 1.0 mM EGTA, pH 7.2 (KOH). Gramicidin (Sigma-Aldrich) was prepared from a stock solution (120 mg/1.0 ml DMSO) to a final concentration of 600 μg/ml of pipette-filling solution. Alternatively, amphotericin B was prepared from a stock solution (6 mg/100 μl DMSO) and added to a final concentration of 120 μg/ml of pipette-filling solution. Pipette tips were filled with a similar solution without gramicidin or amphotericin B. Cells were continuously (between test applications of agonists) perfused with gravity-fed extracellular solution provided by a custom-made pipette positioned 100-200 μm from the studied cell. Computer-controlled exchange to solutions containing agonist via solenoid valves occurred with a time constant of ~50 ms, as measured by the change in offset potential on changing between high and low K^+ concentrations in the perfusate (Karlsson et al., 2011).

Electrophysiological recording

Electrophysiological experiments to study $[Cl^-]_i$ recovery were made by using the gramicidin-perforated patch technique, which enables recording of whole-cell currents without interference with the intracellular Cl^- concentration (Abe et al., 1994; Kyrozis and Reichling, 1995) and without current rundown (Wang et al., 2003). Experiments to estimate resting Cl^- conductance, which depend on estimates of $[Cl^-]_i$ but are compatible with slow Cl^- equilibration with the patch pipette, were made using the quicker amphotericin B-perforated patch technique (Rae et al., 1991). Both perforated-patch techniques are compatible with rapid Cl^- loading (Karlsson et al., 2011). The majority of experiments were made under voltage-clamp conditions, but a few control experiments were made under current-clamp conditions at zero current. Patch pipettes had a resistance of 3-4 MΩ when filled with standard pipette-filling solution and immersed in the standard extracellular solution (see above). Series resistance was evaluated repeatedly during experiments, by the "membrane test" provided in the Clampex software (versions 9 and 10; Molecular Devices), and was typically 15-40 MΩ. Online series-resistance compensation, which can never be complete and is associated with extra noise, was not used. For more complete compensation, all voltages were corrected for series resistance offline with voltage error computed from raw current and series resistance. Liquid-junction potentials were calculated using the Clampex software and have been subtracted in all potentials given. All experiments were performed at room temperature (21-23°C).

Loading cells with Cl^- and estimation of $[Cl^-]_i$ recovery time course

Cells were loaded with Cl^-, to concentrations up to ~70 mM, by using combined depolarization and application of GABA (1.0 mM) or glycine (1.0 mM; Karlsson et al., 2011). Estimates of $[Cl^-]_i$ during loading as well as during recovery after loading were calculated from E_{Cl} as obtained from *I-V* relations constructed from rapid voltage ramps (rate of $\pm$ 1.6 V s^{-1}) during brief applications of GABA or glycine (100 μM to 1.0 mM) and after correction for series resistance and subtraction of leak currents. The studied cells generated stable (for >10 min) responses to GABA as well as to glycine during perforated-patch recordings (Druzin and Johansson, 2016). Since the method used to estimate $[Cl^-]_i$ depends on the current reversal potential, it is not sensitive to changes in the absolute GABA- or glycine-evoked conductance or peak current. Under the conditions used, without HCO_3^- in the solutions, the reversal potentials for currents evoked by GABA or glycine (E_{GABA} and $E_{glycine}$) are equivalent to E_{Cl} (Chavas and Marty, 2003). The probe applications of GABA/glycine were given at a voltage close to the estimated E_{Cl} to minimize influence on $[Cl^-]_i$. The charge transfer associated with a probe application of GABA/glycine was estimated to affect $[Cl^-]_i$ by <1.0 mM, as calculated from the "equivalent volume" of cytosol. The equivalent volume, v_{equ}, was obtained from the Cl^- loading procedure and represented the volume in which the recorded charge transfer, Q, would cause the observed $[Cl^-]_i$ changes, $\Delta[Cl^-]_i$, according to the relation: $v_{equ} = QF^{-1} (\Delta[Cl^-]_i)^{-1}$, where F is the Faraday constant. Thus, v_{equ} corresponds to the expected cytosolic volume (Karlsson et al., 2011). Leak currents, including small voltage-dependent components, were obtained from voltage-ramps given in the absence of GABA and glycine. The obtained leak *I-V* relation (after correction for series resistance) was fitted by a linear function or by the exponential function $I = A + B\, e^{V/C}$ (A, B, and C being constants). The latter function was used to calculate the leak current component when GABA or glycine was present. This procedure takes the differences in voltage, arising as a consequence of the series resistance and different current amplitudes, during ramps with and without GABA/glycine into account, and, therefore, provides a better estimate of leak currents than the commonly used technique to directly subtract the current recorded in the absence of ligand from that recorded in the presence of ligand. The similar results obtained with GABA and with glycine to load cells with Cl^- (Karlsson et al., 2011) show that the method used for loading is not critically influencing the results. Thus, GABA and glycine were here used interchangeably and each agonist was used for estimation of $[Cl^-]_i$ while blocking receptors for the other to clarify their role in $[Cl^-]_i$ regulation.

Derivation of relative Cl^- conductance at rest

Previous methods for estimating the relative Cl^- conductance of the neuronal membrane at rest have not been

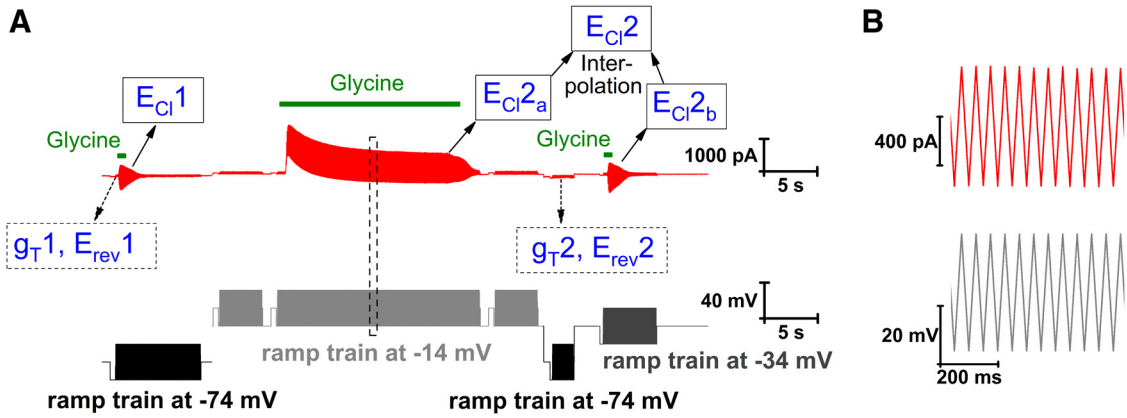

Figure 1. Protocol used for estimation of relative Cl^- conductance at rest. ***A***, Voltage protocol (below in black/gray; ramp sequences appearing as blocks; for detailed ramps, see ***B***) and recorded current (top, red), with glycine application as indicated by the green bars (short bars, 100 μM; long bar, 1.0 mM). ***B***, Voltage protocol (bottom) and recorded current (top) for part of the ramp train shown within dashed box in ***A***.

straight-forward and dependent on many assumptions (Forsythe and Redman, 1988). We here aimed at a method with which we could estimate the relative Cl^- conductance from voltage ramps applied under conditions with different Cl^- concentrations on the in- or outside of the membrane. The starting assumption was that the membrane current reversal potential could be described by the "conductance" version of the Goldman-Hodgkin-Katz equation (Goldman, 1943; Hodgkin and Katz, 1949; see, e.g., Koester and Siegelbaum, 2013):

$$E_{rev} = (g_K/g_T)E_K + (g_{Na}/g_T)E_{Na} + (g_{Cl}/g_T)E_{Cl} \quad (1)$$

where E_{rev} is the reversal potential for the total current, i.e., the resting potential, g is conductance with subscripts T, K, Na, and Cl for total, K^+, Na^+, and Cl^-, respectively, and E_K, E_{Na}, and E_{Cl} are the equilibrium potentials for respective ions. From Equation 1, we obtain

$$g_T E_{rev} - g_{Cl} E_{Cl} = g_K E_K + g_{Na} E_{Na} \quad (2)$$

If we manipulate E_{Cl}, e.g., by loading cells with Cl^- as described above, without changing ion conductances and without changing equilibrium potentials for Na^+ and K^+, then for the two conditions, before (subscript 1) and after (subscript 2) Cl^- loading,

$$g_{T1} E_{rev1} - g_{Cl} E_{Cl1} = g_{T2} E_{rev2} - g_{Cl} E_{Cl2} \quad (3)$$

and if g_T does not change (as was experimentally verified, see below), then

$$g_T E_{rev1} - g_{Cl} E_{Cl1} = g_T E_{rev2} - g_{Cl} E_{Cl2} \quad (4)$$

From Equation 4, we obtain the relative Cl^- conductance:

$$g_{Cl}/g_T = (E_{rev2} - E_{rev1})/(E_{Cl2} - E_{Cl1}) = \Delta E_{rev}/\Delta E_{Cl} \quad (5)$$

The relative Cl^- conductance may thus be obtained from the shift in reversal potential of total current relative to the shift in Cl^- equilibrium potential.

We here used continuous voltage ramp sequences, in a regular zigzag pattern, with application of glycine during part of the ramp sequence (Fig. 1). By this procedure, estimates of conductance and reversal potential were obtained before as well as throughout the glycine application, with a time resolution determined by the ramp cycle frequency, here 20 Hz. The control ramps (i.e., before or in the absence of glycine application) were used to estimate total conductance (g_T) and reversal potential (E_{rev}), but also for subtraction of leak currents from the currents evoked by glycine to estimate (E_{Cl}). A first set of g_T, E_{rev} and E_{Cl} estimates were obtained from voltage ramps symmetrically around a holding potential of –74 mV (i.e., near the resting potential). Subsequently the holding voltage was raised to –14 mV (with ramps symmetrically around this voltage, as indicated in Figure 1) and $[Cl^-]_i$ was raised by glycine (1.0 mM) application for 20 s. E_{Cl} was measured at the end of the 20-s glycine application ($E_{Cl}2_a$ in Figure 1). Next, holding voltage was returned to –74 mV and a second estimate of g_T (g_T2) and E_{rev} ($E_{rev}2$) was obtained. A final estimate of E_{Cl} ($E_{Cl}2_b$) was made with ramps around a holding voltage of –34 mV. A linear interpolation between $E_{Cl}2_a$ and $E_{Cl}2_b$ was used to estimate E_{Cl} at the time of g_T2 (and $E_{rev}2$), to account for $[Cl^-]_i$ changes during this time interval. g_T2 was compared with g_T1 to verify that glycine-activated conductance had decayed and to satisfy the conditions for Equation 4. Variations <30% between the two measurements in the same cell were accepted (to account for fluctuations in resting conductance), and absence of any significant systematic difference was confirmed (see Figure 5 below). These measurements were made with 100 μM Cd^{2+}, to minimize transmitter release from adhering presynaptic terminals, and 30 mM TEA (replacing an equimolar amount of Na^+ in the standard extracellular solution), to minimize voltage-gated K^+ currents, tetrodotoxin (TTX; 2.0 μM), to block voltage-gated Na^+ channels, and with the KCC2 blocker VU0255011-1 (10 μM) to minimize outward Cl^- transport between the times for measuring $E_{Cl}2_a$ and $E_{Cl}2_b$. To relate the derived resting g_{Cl} to the total membrane conductance in the absence of blockers, we also considered

the effect of the used blockers on the total resting conductance g_T. Control experiments showed that the total resting conductance in the presence of all four blockers (TEA, Cd^{2+}, TTX, and VU0255011-1; $n = 14$) was, on average, only 54% ($p = 0.0038$, Mann–Whitney test) of that without blockers ($n = 10$). This effect could be ascribed to TEA and/or Cd^{2+} since the total conductance in a combination of TTX and VU0255011-1 ($n = 14$) was not significantly different from that without blockers ($n = 10$).

Computation of $[Cl^-]_i$ recovery time course

The time course of theoretically expected $[Cl^-]_i$ recovery was computed for a simplified model of a spherical one-compartment cell (Karlsson et al., 2011). The model included Cl^- transport mediated by KCC2 as well as Cl^- current through a leak conductance. $[Cl^-]_i$ was computed numerically according to

$$[Cl^-]_i\,(t + \Delta t) = [Cl^-]_i\,(t) + \Delta[Cl^-]_{i,\,KCC2} + \Delta[Cl^-]_{i,\,conductive} \quad (6)$$

where

$$\Delta[Cl^-]_{i,\,KCC2} = -\Delta t\,\Delta\mu_{K,Cl}\,g_{KCC2}\,v_{equ}{}^{-1} \quad \text{(KCC2-mediated change in } [Cl^-]_i) \quad (7)$$

and

$$\Delta[Cl^-]_{i,\,conductive} = I\Delta t\,F^{-1}\,v_{equ}{}^{-1} \quad \text{(channel-mediated change in } [Cl^-]_i) \quad (8)$$

t is time, Δt is the integration time step (here, 50 ms), g_{KCC2} is a transport proportionality factor ("apparent conductance", dependent on the number and transport capacity of KCC2 molecules) for KCC2, $\Delta\mu_{K,Cl}$ is the driving force for KCC2:

$$\Delta\mu_{K,Cl} = RT\,(\ln([Cl^-]_i/[Cl^-]_o) + \ln([K^+]_i/[K^+]_o)), \quad (9)$$

and

$$I = g_{Cl}\,(V_m - E_{Cl}) \quad (Cl^- \text{ leak current}), \quad (10)$$

F is the Faraday constant and v_{equ} is the equivalent volume, i.e., the cytosolic volume where Cl^- equilibrates, taken to be 50% of the total cell volume (here, assumed $5.0\ 10^{-13}$ l, i.e., 50% of the volume of a sphere of radius 6.2 μm; cf Karlsson et al., 2011). The proportionality factor g_{KCC2} was adjusted to match KCC2-mediated $[Cl^-]_i$ recovery to experimental results (experiments with minimized influence of g_{Cl}, compare Fig. 2*F*), whereas g_{Cl} was as experimentally recorded (compare Figure 5 below). The computations were made using Turbo Basic software (Borland).

Statistical analysis

Data are presented as the mean ± SEM, with n representing the number of cells studied. Differences between groups were analyzed with the paired Wilcoxon signed-rank test for paired data and with the Mann–Whitney test for unpaired data; $p < 0.05$ was considered statistically significant. Statistical analyses were performed using the software OriginPro 2016 (OriginLab).

Results

Transporter-dependent recovery of $[Cl^-]_i$

To obtain an overall view of the $[Cl^-]_i$ recovery capacity in dissociated medial preoptic nucleus (MPN) neurons, we first addressed transporter-dependent recovery after a Cl^- load to concentrations significantly above baseline $[Cl^-]_i$, previously estimated to ~9 mM in this preparation (Karlsson et al., 2011). To estimate the capacity, we loaded the cells with Cl^- by combined depolarization and GABA or glycine application. This resulted in an exponential (time constant 3.8 ± 0.4 s, $n = 19$) increase in $[Cl^-]_i$ to 60 ± 3 mM ($n = 19$; Fig. 2*A-C*). After loading, $[Cl^-]_i$ recovery was studied by voltage ramps (to estimate E_{Cl}) given from a holding potential that was kept as close as possible to the gradually changing E_{Cl}, to minimize influence of passive conductive recovery and also to minimize influence of the GABA/glycine applications during recovery (Fig. 2*D*,*E*). This required test runs to obtain a rough estimate of the E_{Cl} recovery time course. Under these conditions, favoring mainly nonconductive, transporter-dependent changes, $[Cl^-]_i$ recovery varied somewhat between cells, following a roughly exponential, a doubly exponential or a nearly linear time course (Fig. 2*F*). For simplicity, we used the best fitted single-exponential for comparison between cells and recording conditions. In control conditions, the time constant was 499 ± 49 s ($n = 19$). Since the recovery time course was considerably slower than estimated for some other cell types, and with other techniques (Staley and Proctor, 1999; Wagner et al., 2001; Földy et al., 2010; Rinke et al., 2010; Deisz et al., 2011), we made a few recordings from neurons dissociated from the CA1 region in brain slices containing the hippocampus. However, in the three hippocampal cells tested, $[Cl^-]_i$ recovery occurred with a time constant of 1877 ± 60 s, thus even slower than for the MPN neurons.

To verify that the $[Cl^-]_i$ recovery described was mediated by transporter activity, we applied several types of blockers. The time course of recovery was not significantly affected by a blocker (bumetanide, 10 μM) of the Na^+-K^+-Cl^- cotransporter 1 (NKCC1; Fig. 3*A*,*D*) but was dramatically slowed by furosemide (0.5 mM; Fig. 3*B*,*D*), which affects also KCC2, as well as by the selective KCC2 blocker VU0255011-1 (10 μM; Fig. 3*C*,*D*). These effects are consistent with the idea that a major fraction of the observed recovery is mediated by KCC2. The kinetic details of transporter-dependent $[Cl^-]_i$ recovery were not investigated further here.

Passive, conductive recovery of $[Cl^-]_i$

If a substantial conductive component contributes to $[Cl^-]_i$ recovery, this should be seen as a voltage-dependent component. KCC2-mediated Cl^- transport does not depend on voltage (see, e.g., Alvarez-Leefmans and Delpire, 2009). We therefore studied $[Cl^-]_i$ recovery as above, but with membrane voltage kept at either –14 or –74 mV during the recovery phase. Test pulses of GABA/

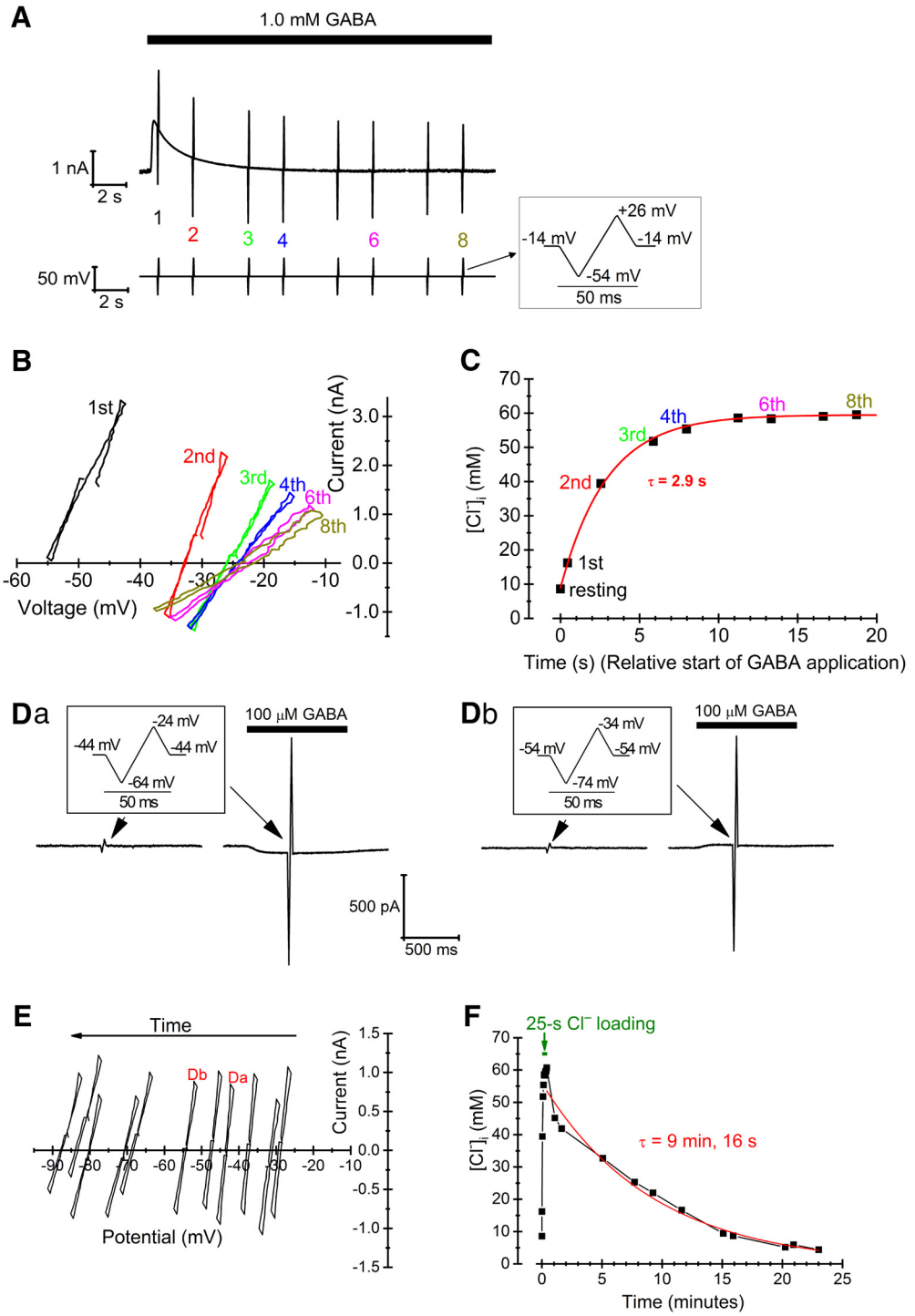

Figure 2. $[Cl^-]_i$ loading and estimation of transporter-dependent recovery capacity. ***A***, Voltage protocol (bottom) and recorded current (top) during loading a cell with Cl^-. Note that the baseline voltage during loading was –14 mV to obtain a large driving force for Cl^- current evoked by 1.0 mM GABA. Data from numbered ramps are shown in ***B*** and ***C***. ***B***, *I-V* relations corresponding to the ramps (no 1-4, 6, 8, as marked in ***A***) applied during Cl^- loading (corrected for series resistance and with leak components subtracted). ***C***, Time course of $[Cl^-]_i$ during Cl^- loading, as computed from E_{Cl} obtained from the *I-V* relations in ***B***, and superimposed fitted exponential curve. Resting $[Cl^-]_i$ was obtained from a separate, preceding ramp (not shown). ***D***, Voltage ramps (insets), leak and GABA-evoked currents used to probe $[Cl^-]_i$ during recovery after the end of Cl^- loading. Ramps for $[Cl^-]_i$ estimates at two different times are shown in ***Da*** and ***Db*** (compare *I-V* relations in ***E***). ***E***, *I-V* relations from probe currents as in ***D*** (with the relations corresponding to currents in ***Da*** and ***Db*** indicated). Note that *I-V* relations are shifted with time to more negative voltages, as a consequence of the changing $[Cl^-]_i$ and E_{Cl}. ***F***, Full-time course of $[Cl^-]_i$ changes during loading (first 25 s) and recovery phases with superimposed mono-exponential fit (red thick line) of the recovery phase.

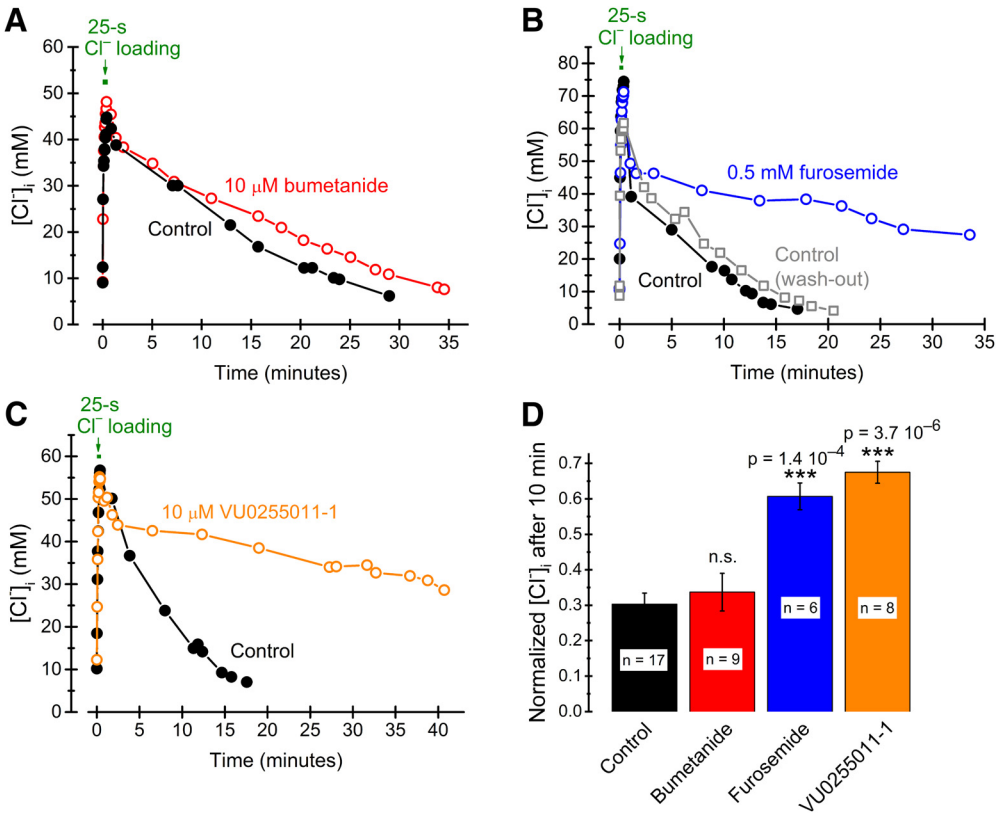

Figure 3. Pharmacology of transporter-mediated recovery of $[Cl^-]_i$. ***A–C***, $[Cl^-]_i$ recovery under control conditions (black filled circles) and in the presence of 10 μM bumetanide (***A***, red open circles), 0.5 mM furosemide (***B***, blue open circles), and 10 μM VU0255011-1 (***C***, orange open circles), with control and drug application for the same cell. Cl^- was loaded and $[Cl^-]_i$ quantified as in Figure 2. ***D***, Summary of drug effects on the level of $[Cl^-]_i$ after 10 min recovery, measured as $[Cl^-]_i$ normalized to maximal $[Cl^-]_i$ during Cl^- loading. Note the lack of significant effect of the NKCC1-blocker bumetanide but highly significant effects of the KCC2 blockers furosemide and VU0255011-1.

glycine were still applied at a holding voltage close to E_{Cl}, to minimize GABA/glycine-induced Cl^- flux. The time at these voltages was, however, very small compared with the total recovery time. The recovery time constant observed at –14 mV was 843 ± 208 s (n = 8), significantly (p = 0.0078; paired Wilcoxon signed-rank test) longer than that at –74 mV (375 ± 95 s; n = 8) in the same cells. The difference obtained by changing the holding voltage was reversible (Fig. 4*A*,*B*). In addition, $[Cl^-]_i$ recovered to a lower level (4.3 ± 1.2 mM, n = 8) at –74 mV than at –14 mV (10.9 ± 3.0 mM; n = 8; p = 0.039; evaluated from the asymptote of the fitted exponential function). Thus, the data are compatible with a substantial contribution of conductive Cl^- flux to $[Cl^-]_i$ recovery.

To quantify the conductive component of $[Cl^-]_i$ recovery in isolation, we repeated the experiments with different holding voltages in the presence of the KCC2 blocker VU0255011-1 (10 μM): There was only little recovery (7.9 ± 2.7% of the loaded $[Cl^-]_i$ recovered after 20 min; n = 5) at –14 mV, whereas at –74 mV, $[Cl^-]_i$ recovered with a time constant of 651 ± 171 s (n = 5) and 60 ± 5% of the $[Cl^-]_i$ increase during loading was eliminated after 20 min of recovery (Fig. 4*C*,*D*). Thus, it is clear that without KCC2 there is very small, if any, Cl^- extrusion capacity to counteract the effect of conductive Cl^- transport on $[Cl^-]_i$ at –14 mV and that at –74 mV, conductive Cl^- transport accounts for a recovery time course in the same order of magnitude as does KCC2 in the absence of blockers (compare Fig. 3, black filled symbols, with Fig. 4*D*, brown filled symbols).

Estimate of resting Cl^- conductance

From above, it is clear that although KCC2 is required for a rapid and complete recovery of $[Cl^-]_i$ to normal resting levels, a significant recovery takes place also by passive, conductive pathways in the absence of functional KCC2. The rate of such recovery will depend on the conductance to Cl^-, g_{Cl}. Resting g_{Cl} will also be an important determinant of resting $[Cl^-]_i$ (Johansson et al., 2016). We therefore derived a method for estimating the resting g_{Cl}, as described in Materials and Methods and Figure 1. Since the method depends on a total membrane conductance, g_T, that does not change with Cl^- loading, we first verified that g_T before (g_T1) and shortly after (g_T2) Cl^- loading was not significantly different (Fig. 5*A*). Subsequently, we computed the relative resting g_{Cl}, from Equation 4 and the conductance and reversal potential measures obtained as described in Figure 1. A final computation accounted for the effect of used background blockers (TEA, Cd^{2+}, TTX, and VU0255011-1) on the total membrane conductance (see Materials and Methods). The obtained relative resting g_{Cl} was 6.0 ± 1.4% (n = 12; relative to total resting conductance in the absence of

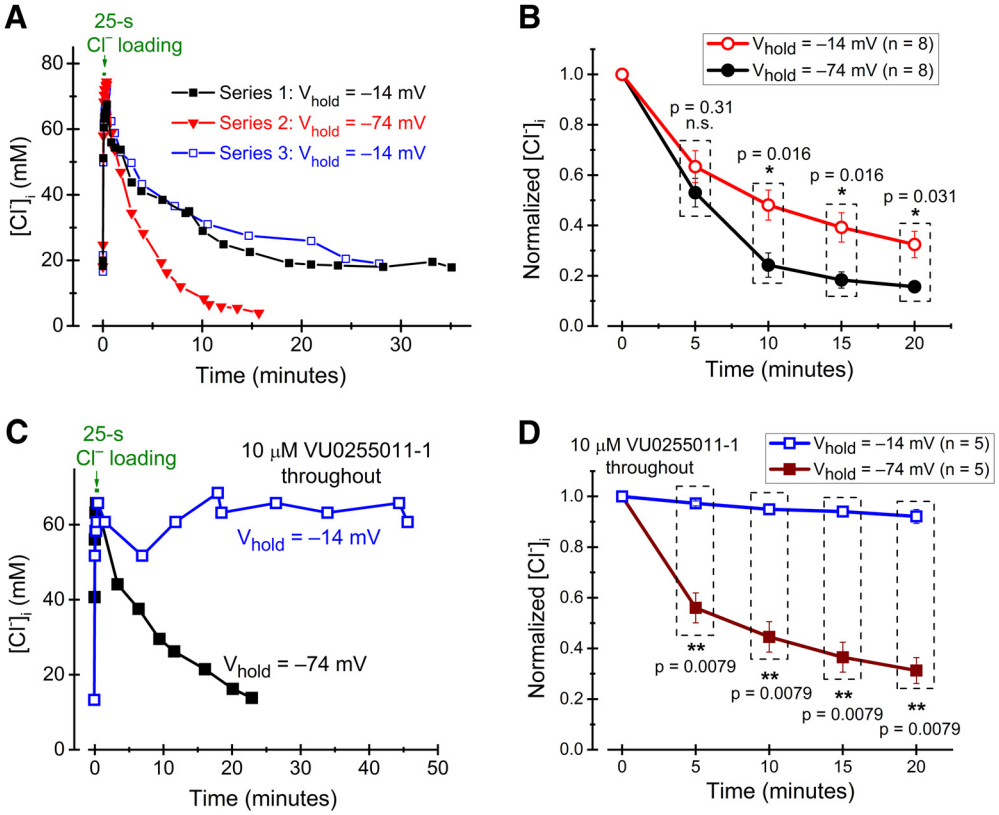

Figure 4. Effect of voltage on $[Cl^-]_i$ recovery. ***A***, $[Cl^-]_i$ recovery in an individual cell at two different levels of holding voltage, as indicated, in control solution. Note that $[Cl^-]_i$ recovers quicker and to a lower concentration at –74 mV compared with at –14 mV. ***B***, Summary of data showing $[Cl^-]_i$ recovery at –74 and at –14 mV (as in ***A***) in eight neurons. ***C***, $[Cl^-]_i$ recovery in an individual cell at two different levels of holding voltage, as indicated, in the presence of 10 μM VU0255011-1. ***D***, Summary of data showing $[Cl^-]_i$ recovery at –74 and at –14 mV in the presence of 10 μM VU0255011-1 (as in ***C***) in five neurons. Probe pulses to estimate $[Cl^-]_i$ were given at slightly different times during each recovery interval (to keep the membrane potential close to E_{Cl}). To compare at similar times, in ***B*** and ***D***, interpolation was used for data pairs closest to the time points illustrated, and $[Cl^-]_i$ was normalized to the maximal concentration during loading.

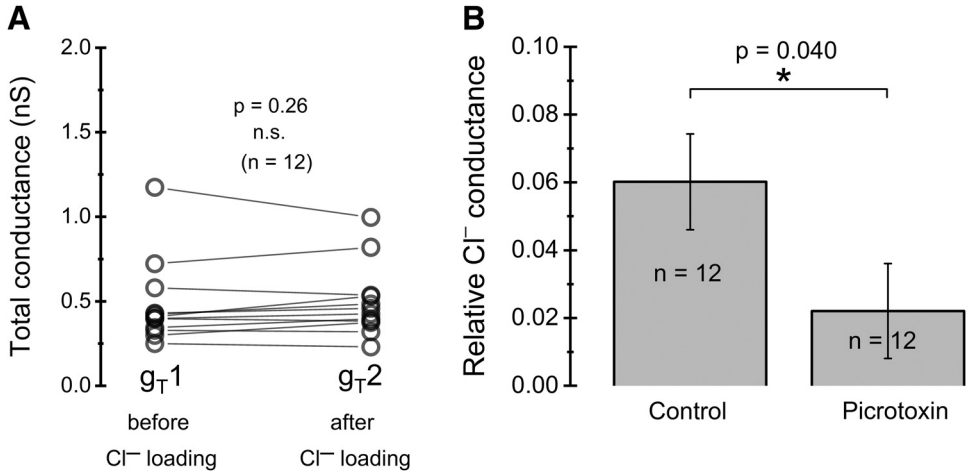

Figure 5. Relative resting Cl^- conductance. ***A***, Distribution of measured total conductances (in the presence of VU0255011-1, TTX, Cd^{2+}, and TEA; see main text), showing no significant difference before and after Cl^- loading, as required for the method used to estimate resting Cl^- conductance. Data paired for individual cells. ***B***, Relative resting Cl^- conductance, in control conditions and in the presence of 100 μM PTX. Note that the given values in ***B*** are relative to the total membrane conductance in the absence of blockers.

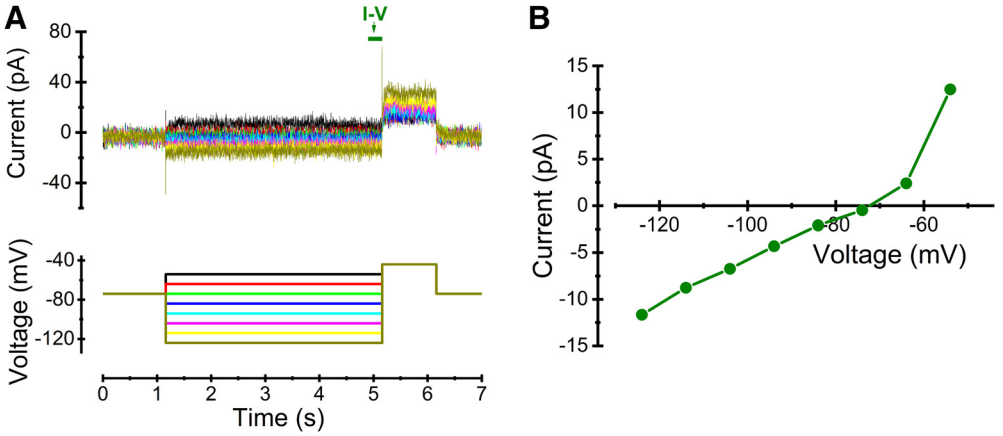

Figure 6. Lack of ClC-2 currents. ***A***, Voltage protocol (bottom) used for detecting ClC-2 currents and corresponding currents (top) recorded in an MPN neuron. Colors of individual current traces matches the colors in the voltage protocol. ***B***, *I-V* relation for the currents in ***A*** (average amplitude during the time marked by olive bar in ***A***). Note the small amplitude and the linearity in the range below −65 mV.

blockers), corresponding to an absolute resting g_{Cl} of 54 ± 13 pS (n = 12).

We next addressed the molecular basis for the resting g_{Cl}. We first tested the hypothesis that open $GABA_A$ receptors accounted for part of g_{Cl}. Relative resting g_{Cl} obtained from experiments with PTX (100 μM) added to the external solution was only 2.2 ± 1.4% (n = 12; Fig. 5*B*), or ~37% of that without PTX. Since 200 μM PTX does not significantly affect the near-steady glycine-evoked current in the studied cell type (Karlsson et al., 2011), this suggests that $GABA_A$ receptors account for a major fraction of resting g_{Cl}.

ClC-2 channels do not contribute significantly to resting conductance in MPN neurons

Because Cl^--permeable ClC-2 channels have been reported to contribute substantially to the resting conductance in CA1 pyramidal cells (Rinke et al., 2010), we used a voltage protocol suitable for detection of Cl^- currents through ClC-2 channels (Fig. 6*A*, bottom) to establish whether the MPN neurons express such channels. However, the current responses in eight cells tested were only composed of linear capacitive and small leak currents in the relevant voltage range (Fig. 6*A*, top, *B*), making it unlikely that ClC-2 contributes significantly to the resting conductance in MPN neurons.

Contribution of $GABA_A$ receptors to conductive $[Cl^-]_i$ recovery

The above results show that there is a significant resting Cl^- conductance in MPN neurons and suggest that a major fraction of this conductance is due to $GABA_A$ receptors. We therefore expected that $GABA_A$ receptors may contribute to $[Cl^-]_i$ recovery after a high Cl^- load. In dissociated MPN neurons, $GABA_A$ receptors may be activated as a consequence of spontaneous GABA release from adhering presynaptic nerve terminals (Haage et al., 1998). We speculated that possibly such spontaneous GABA release could contribute to g_{Cl} and $[Cl^-]_i$ recovery. To clarify this, we studied the time course of conductive $[Cl^-]_i$ recovery (i.e., in the presence of 10 μM VU0255011-1 to block KCC2) under voltage-clamp conditions at –74 mV. A few control recordings showed that in the absence of additional blockers, a roughly similar time course of $[Cl^-]_i$ recovery is seen under current-clamp conditions at zero current (Fig. 7*A*). We first compared $[Cl^-]_i$ recovery at –74 mV without and with TTX (2.0 μM) to block action potential-evoked release of GABA, however, without noting any significant difference (Fig. 7*A*). We subsequently added 3.0 μM gabazine (SR-95531 hydrobromide), previously shown to block spontaneous IPSCs in the studied cell type (Karlsson et al., 2011), but also this was without significant effect on conductive $[Cl^-]_i$ recovery, as was also the glycine-receptor blocker strychnine (10 μM; Fig. 7*A*). The lack of effect of gabazine was somewhat surprising in light of the above suggested contribution of $GABA_A$ receptors to resting g_{Cl}. However, while PTX, which was used above for resting g_{Cl}, is noncompetitive and usually considered as a pore blocker (Takeuchi and Takeuchi, 1969; Etter et al., 1999), gabazine is a competitive $GABA_A$ receptor antagonist (Heaulme et al., 1986; Hamann et al., 1988) and may fail to block receptor-channels that are spontaneously open in the absence of GABA (Birnir et al., 2000; Wlodarczyk et al., 2013). Indeed, consistent with the effect of PTX on resting g_{Cl}, PTX significantly reduced conductive $[Cl^-]_i$ recovery in the studied 10-min interval (Fig. 7*B*), suggesting that spontaneously open $GABA_A$ receptors in the absence of GABA do contribute to recovery.

Neurosteroid regulates conductive $[Cl^-]_i$ recovery via miniature IPSCs (mIPSCs)

Although the above results suggested that spontaneous, action potential-independent GABA release does not significantly affect $[Cl^-]_i$ recovery, we hypothesized that such release and the generated mIPSCs may still play a physiologic role for the Cl^- homeostasis. Hypothetically, mIPSC potentiation by an endogenous modulator may enable such a functional role for the spontaneously released transmitter. The endogenous neurosteroid 3α-hydroxy-5α-pregnane-20-one (allopregnanolone), which may be produced *de novo* in the brain, e.g., during stress

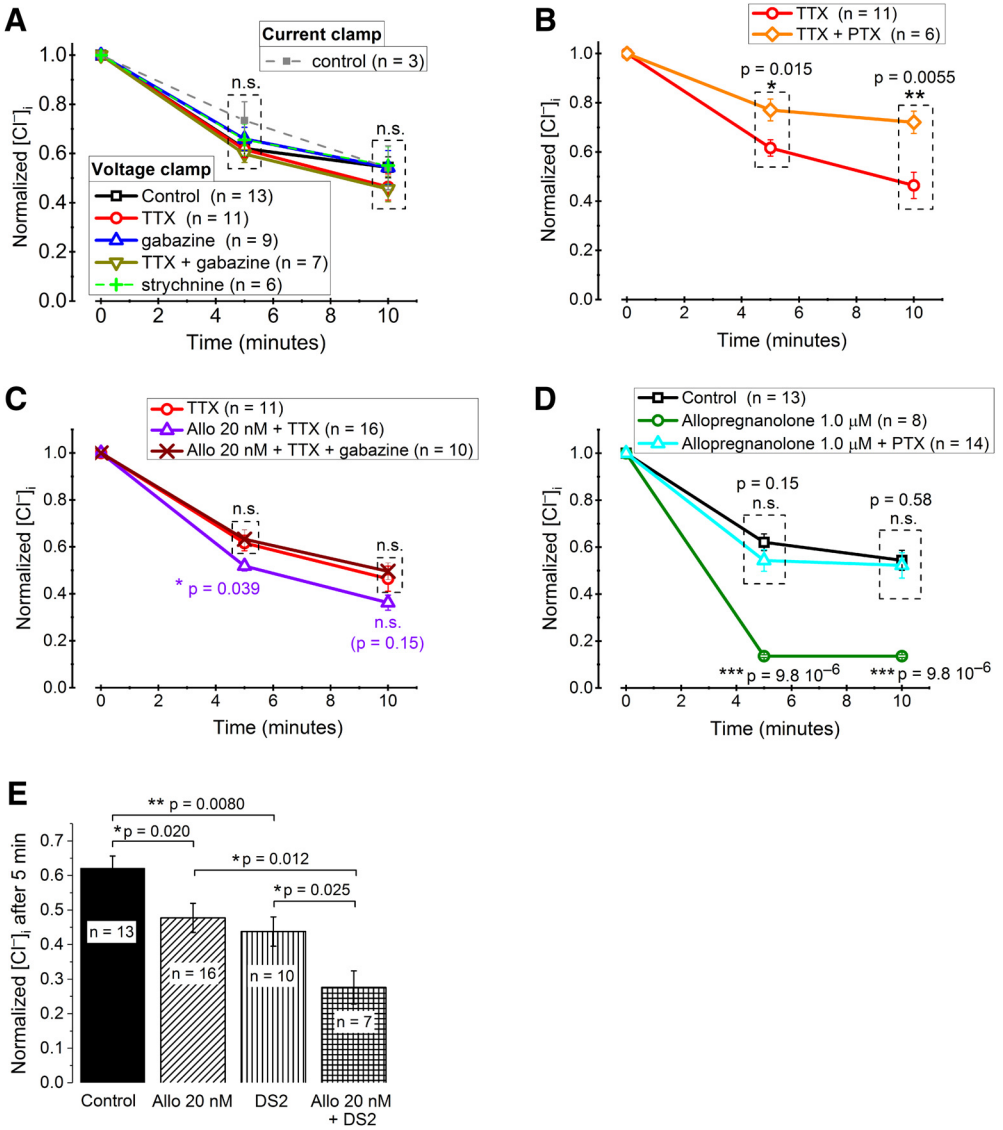

Figure 7. Role of spontaneously open $GABA_A$ receptors and of neurosteroid-potentiated mIPSCs for $[Cl^-]_i$ recovery. ***A***, Relative $[Cl^-]_i$, illustrating recovery 5 and 10 min after Cl^- loading. Current-clamp (0 pA) between test ramps during recovery phase: control only. Voltage-clamp (–74 mV) between test ramps during recovery phase: control, 2.0 μM TTX, 3.0 μM gabazine, a combination of TTX and gabazine, or 10 μM strychnine, as indicated. Note the lack of significant differences. ***B***, Relative $[Cl^-]_i$ (as in ***A***, voltage-clamp only), with significantly reduced recovery in the presence of 100 μM PTX. ***C***, Relative $[Cl^-]_i$ (as in ***B***), showing gabazine-sensitive enhancement of recovery in the presence of 2.0 μM TTX and the neurosteroid allopregnanolone (Allo) in a concentration (20 nM) known to enhance mIPSC frequency and prolong mIPSC decay. ***D***, Relative $[Cl^-]_i$ (as in ***B***) showing the dramatic enhancement of $[Cl^-]_i$ recovery by allopregnanolone in a concentration (1.0 μM) that may directly activate $GABA_A$ receptors and the block of this effect by 100 μM PTX. ***E***, Comparison of the effects of 20 nM Allo, DS2 and a combination of Allo and DS2 on normalized $[Cl^-]_i$ after 5 min of recovery from a Cl^- load as in ***A***–***D***. Note the highly significant effect of DS2 and the additive effects of Allo and DS2. To compare data recorded at slightly different times in ***A***–***E***, interpolation was used for data pairs closest to the time points illustrated and $[Cl^-]_i$ was normalized to the maximal concentration during loading.

(Purdy et al., 1991), increases the frequency as well as prolongs the decay time of mIPSCs in MPN neurons (Haage and Johansson, 1999). We therefore analyzed the effect of allopregnanolone on $[Cl^-]_i$ recovery at –74 mV in the presence of 10 μM VU0255011-1 to block KCC2. It was clear that, in the presence of TTX (2.0 μM) to block action potential-evoked GABA release, 20 nM allopregnanolone, a concentration that mainly affects the time course of mIPSCs (Haage et al., 2002) and may be reached *in vivo* (Purdy et al., 1991), significantly potentiated $[Cl^-]_i$ recovery as quantified 5 min after loading with Cl^- (Fig. 7*C*). This effect of allopregnanolone was abolished by gabazine (3.0 μM; Fig. 7*C*), suggesting that the steroid effect was mediated by $GABA_A$ receptors that were activated by GABA, as expected for mIPSCs. Allopregnanolone at 20 nM concentration did not affect the baseline current in 11 cells tested ($p = 0.55$; paired sample Wilcoxon signed-rank test), ruling out significant ef-

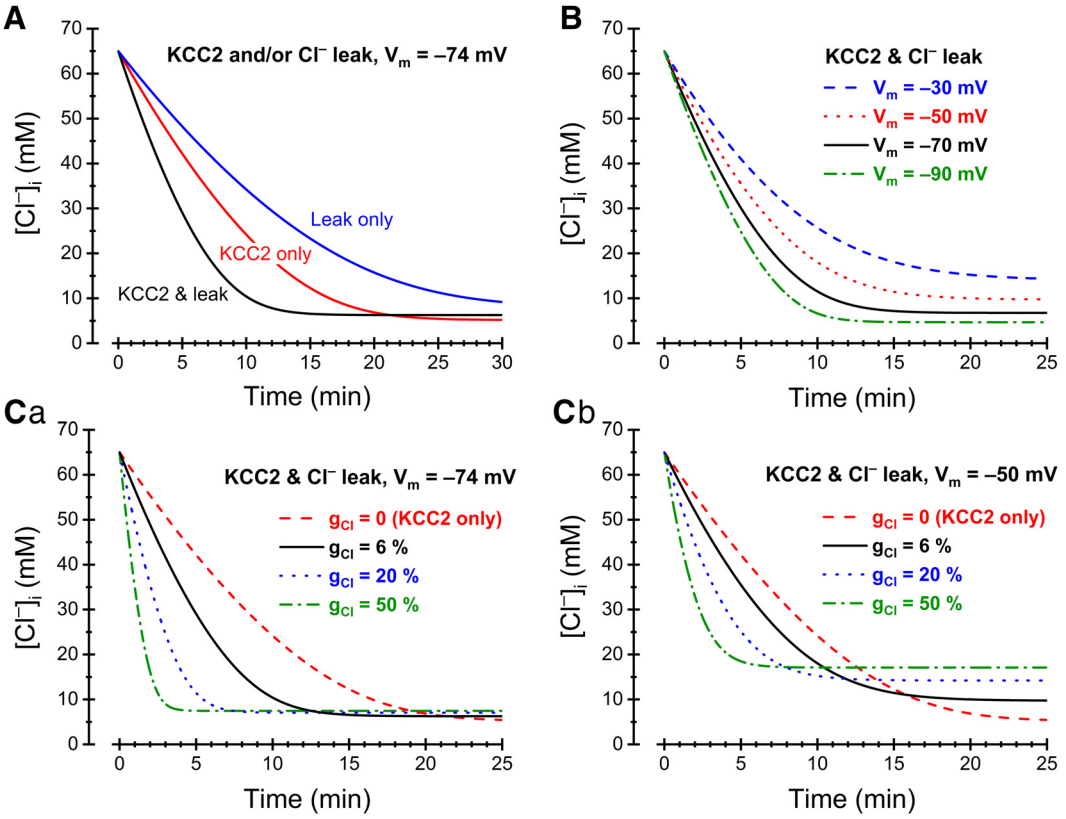

Figure 8. Computed $[Cl^-]_i$ recovery. Dependence on g_{Cl}, g_{KCC2}, and V_m. ***A***, Recovery mediated by KCC2 only (red, middle), Cl^- leak only (blue, top), or a combination of KCC2 and Cl^- leak (black, bottom) at V_m = –74 mV. ***B***, Recovery mediated by KCC2 and Cl^- leak in combination at different V_m, as indicated. Note that the rate of recovery as well as the asymptotic steady-state $[Cl^-]_i$ depends on V_m. ***C***, Recovery mediated by KCC2 and Cl^- leak in combination at different relative g_{Cl}, as indicated and at V_m = –74 mV (***Ca***) or V_m = –50 mV (***Cb***). Note that the speed of recovery increases with g_{Cl} and that the asymptotic steady-state $[Cl^-]_i$ also increases with g_{Cl}. The latter effect is weak at –74 mV (***Ca***) but prominent at –50 mV (***Cb***). The transport capacity of KCC2 in (***A–C***) was adjusted by setting the transporter proportionality factor (apparent conductance; Johansson et al., 2016) g_{KCC2} to 6.7 10^{-21} mol^2 V^{-1} C^{-1} s^{-1}, to match modeled KCC2-mediated $[Cl^-]_i$ recovery time course to experimental results.

fects on tonic $GABA_A$ receptor-mediated currents at this steroid concentration.

Higher, micromolar concentrations of allopregnanolone may directly activate $GABA_A$ receptors in MPN neurons (Haage and Johansson, 1999). Here, the effect of 1.0 μM allopregnanolone on $[Cl^-]_i$ recovery was dramatic and highly significant (Fig. 7*D*, compare top and lower curves). The effect was abolished in the presence of 100 μM PTX, confirming an action on $GABA_A$ receptors (Fig. 7*D*).

It seems possible that some of the effect of 1.0 μM allopregnanolone may be mediated by δ-subunit-containing $GABA_A$ receptors, which are extra- or perisynaptically located and highly sensitive to potentiation by neuroactive steroids (Stell et al., 2003). They may also display a degree of spontaneous activity (Jensen et al., 2013; Wlodarczyk et al., 2013) that should contribute to the background Cl^- conductance. We took advantage of the positive allosteric modulator δ-selective compound 2 (DS2; Wafford et al., 2009; Jensen et al., 2013), which, although not perfectively selective, may preferentially potentiate δ-subunit-containing $GABA_A$ receptors at concentrations <2 μM (Ahring et al., 2016). Here, DS2 (1.0 μM) significantly enhanced the $[Cl^-]_i$ recovery as measured 5 min after loading with Cl^- (Fig. 7*E*), suggesting that $[Cl^-]_i$ recovery may be pharmacologically enhanced via positive modulation of δ-subunit-containing $GABA_A$ receptors. This effect was additive to the effect of 20 nM allopregnanolone (Fig. 7*E*).

Theoretically expected influence of conductive Cl^- flux on $[Cl^-]_i$ recovery

The experimental results described above show that MPN neurons display a resting Cl^- conductance that contributes significantly to recovery of $[Cl^-]_i$ after a high Cl^- load. To clarify the theoretically expected contribution of the resting g_{Cl} to $[Cl^-]_i$ recovery, we used the model described by Karlsson et al. (2011) to compute the time course of $[Cl^-]_i$. In essence, the influence of relative g_{Cl} and of the KCC2-mediated transport capacity (g_{KCC2}) was analyzed in a single-compartment cell with dimensions, total resting conductance and ion (external K^+ and Cl^-, internal K^+) concentrations matching experimental values (see Materials and Methods). The time course of computed $[Cl^-]_i$ recovery mediated by KCC2 in the absence of resting g_{Cl} was matched to the experimental results (Fig. 2*F*, control; experiment with minimized influence of g_{Cl}) by adjusting g_{KCC2} (Fig. 8*A*, red, middle).

Assuming a relative resting g_{Cl} of 6.0% (of a total conductance of 0.89 nS in blocker-free conditions, to match the experimentally obtained conductance of 0.48 nS in Figure 5*A*, left, and the effect of the used blockers on g_T as described in Materials and Methods), but no KCC2-mediated transport resulted in a computed $[Cl^-]_i$ recovery (at –74 mV) that reasonably well matched the experimental recovery (Fig. 4*D*, lower curve) observed with KCC2 blocked (Fig. 8*A*, blue, top). The computed $[Cl^-]_i$ recovery with g_{Cl} as well as KCC2-mediated transport (Fig. 8*A*, black, bottom) was quicker, showing that even with a relative resting g_{Cl} as low as 6.0%, a substantial effect on $[Cl^-]_i$ is indeed expected. It is also clear that $[Cl^-]_i$ settles at a slightly higher steady level due to the combined effects of g_{Cl} and KCC2 as compared with KCC2-mediated transport only (Fig. 8*A*, black, bottom). It was recently shown that, in a cell where $[Cl^-]_i$ is determined by g_{Cl} and g_{KCC2}, at steady-state, E_{Cl} will settle between the membrane potential and the equilibrium potential for K^+, depending on the relative influence of g_{Cl} and of g_{KCC2} (Johansson et al., 2016). As shown here (Fig. 8*B*), the membrane potential (V_m) influences the rate of $[Cl^-]_i$ recovery as well as the steady-state $[Cl^-]_i$. As g_{Cl} drives E_{Cl} toward V_m, there is a trade-off between the rate of $[Cl^-]_i$ recovery (maximal at high g_{Cl}) and the steady-state $[Cl^-]_i$ (minimal at low g_{Cl}). The effect of g_{Cl} on steady-state $[Cl^-]_i$ is small at strongly negative V_m (–74 mV; Fig. 8*Ca*) but prominent at less negative V_m (–50 mV; Fig. 8*Cb*). It is clear from Figure 8*C* that, at more negative potentials in particular, there is a strong potential to modulate the rate of $[Cl^-]_i$ recovery by substances that affect g_{Cl}, such as neuroactive steroids or $GABA_A$ receptor active compounds like DS2 and PTX. At more positive potentials, in particular, there is also a potential to modulate resting $[Cl^-]_i$ by such substances.

Discussion

In the present study, we have used voltage-ramp techniques to analyze how passive, conductive Cl^- flux contributes to $[Cl^-]_i$ recovery after a significant Cl^- load introduced in central neurons. We have also compared with $[Cl^-]_i$ recovery mediated by the transporter KCC2 and showed that conductive flux may account for a contribution in the same order of magnitude as KCC2. To estimate the relative resting Cl^- conductance, for which little information is available concerning central mammalian neurons, we developed a novel technique based on $[Cl^-]_i$ perturbation. We showed a relative resting Cl^- conductance of 6%, with a major fraction mediated by open $GABA_A$ receptors. We also showed that conductive $[Cl^-]_i$ recovery may be dramatically potentiated by the endogenous neurosteroid allopregnanolone, acting by enhancing the frequency and prolonging the time course of miniature postsynaptic currents. This suggests a novel role for neurosteroids in Cl^- homeostasis as well as a novel role for spontaneous transmitter release.

KCC2-mediated $[Cl^-]_i$ recovery in isolated preoptic neurons

The time constant of $[Cl^-]_i$ recovery in the studied MPN neurons was considerably longer than the few seconds reported in some earlier studies (Staley and Proctor, 1999; Wagner et al., 2001; Földy et al., 2010; Rinke et al., 2010; Deisz et al., 2011), including studies of hippocampal CA1 neurons, where whole-cell recording or sharp microelectrodes were used. The recordings we made from hippocampal neurons showed a still slower $[Cl^-]_i$ recovery, suggesting that the difference from the earlier studies did not depend on the cell type, but likely on the recording techniques or type of preparational procedures. It seems likely that earlier studies with sharp microelectrodes or whole-cell recording may not have fully accounted for the introduced Cl^- leak to/from the outside or equilibration with the patch pipette, the latter which may occur within a few seconds (Pusch and Neher, 1988). Further, the negative holding voltage used in some studies implies that conductive $[Cl^-]_i$ recovery may have contributed significantly, whereas we reduced influence of conductive recovery by changing the holding voltage gradually while transporter-mediated recovery was estimated. Indeed, studies using the gramicidin-perforated patch technique report a slower recovery (>30 s up to several minutes; Chabwine et al., 2004; Lee et al., 2011; Pellegrino et al., 2011). Also measurements with optical Cl^- sensors suggest a recovery time constant of ~30 s (Berglund et al., 2006) or several minutes (Friedel et al., 2015), although conductive recovery may have contributed also there. On the other hand, possibly the KCC2-mediated transport is dependent on the naturally surrounding milieu, which was largely eliminated by the dissociation process in the present work. Clearly, dendrites were removed in the present study. The $[Cl^-]_i$ fluctuations in dendrites are expected to be much quicker than in the cell body (Doyon et al., 2011). Therefore, the presently reported time course of $[Cl^-]_i$ recovery should be interpreted as reflecting the KCC2-dependent transport capacity of isolated neuronal cell bodies.

Conductive $[Cl^-]_i$ recovery

For any cell with a significant Cl^- permeability, a raised cellular $[Cl^-]_i$ is expected to recover by conductive pathways to a level determined in part by the membrane potential. To our knowledge, such recovery has previously not been rigorously quantified. We here showed that, surprisingly, conductive $[Cl^-]_i$ recovery at negative holding potentials was substantial, with a time course roughly similar to the time course of isolated KCC2-dependent recovery. This implies that the gain in speed of recovery contributed by KCC2 is not dramatic, if a sufficiently negative resting potential can be maintained. Nevertheless, KCC2 has been shown important for nervous function, with reduced KCC2 function being associated with several types of pathology, such as neuropathic pain (Coull et al., 2003), epilepsy (Huberfeld et al., 2007), autism (Tyzio et al., 2014; Merner et al., 2015), schizophrenia (Merner et al., 2015), spasticity (Boulenguez et al., 2010), and ischemia (Jaenisch et al., 2010). There are several possibilities as to why KCC2 may be needed despite substantial conductive recovery. First, conductive recovery is dependent on the membrane potential, V_m. Thus, when V_m is raised, e.g., as a consequence of ongoing excitatory synaptic activity, conductive Cl^- flux will drive

$[Cl^-]_i$ toward a higher level, where E_{Cl} equals the momentary V_m. In this respect, conductive Cl^- flux may contribute to loading of Cl^- at raised V_m (as it does during the loading procedure used in the present work). Thus, KCC2 may be crucial in conditions of raised V_m. Second, even at the resting potential in the absence of synaptic depolarization, conductive $[Cl^-]_i$ recovery cannot lower E_{Cl} beyond the membrane potential, and thus not sufficiently to produce hyperpolarizing GABA or glycine responses. The slight HCO_3^- permeability of $GABA_A$ and glycine receptors implies that extra lowering of E_{Cl} is needed for hyperpolarizing responses. Although GABA and glycine could still mediate shunting inhibition, it seems possible that hyperpolarizing responses may be of advantage in some conditions, due, e.g., to the different distribution in time and space of hyperpolarization and the underlying conductance change (Kaila et al., 2014). Third, the contribution by KCC2 to $[Cl^-]_i$ recovery, even if small, still may be crucial to normal neural function. The finding that even mild KCC2 hypofunction may degrade neural coding (Doyon et al., 2016a) supports this possibility. Since conductive $[Cl^-]_i$ recovery may be of a similar magnitude as KCC2-dependent recovery, it seems likely that it will also be critical for neural coding and that reduced conductive recovery may be associated with pathology. Further, the potential for modulation of $[Cl^-]_i$ recovery via altered g_{Cl}, as illustrated in Figure 8*Ca*, suggests that the levels of neuroactive steroids or the presence of other $GABA_A$ receptor active substances, such as DS2, may be expected to affect the degree of disturbance in $[Cl^-]_i$-related pathologic conditions.

The expression of Cl^- transporters and $[Cl^-]_i$ change during development, with fetal and early postnatal stages dominated by a low expression of KCC2, but a relatively high expression of NKCC1 and a relatively high $[Cl^-]_i$ (see, e.g., Ben-Ari, 2002). If $[Cl^-]_i$ is to be maintained lower than dictated by the thermodynamic equilibrium for NKCC1 (usually >60 mM), NKCC1 must be opposed by outward Cl^- flux. In the absence of Cl^- extruding transporters, the resting g_{Cl} in combination with a negative resting potential may account for such outward Cl^- flux. Thus, we may expect that conductive $[Cl^-]_i$ recovery plays a relatively larger role early in development and in other situations when KCC2 expression is low, compared with when KCC2 expression is high.

Resting Cl^- conductance

The rate of conductive $[Cl^-]_i$ change will necessarily depend on the membrane Cl^- conductance, g_{Cl}. Neuronal membranes are permeable to Cl^- even at rest (Russell and Brown, 1972; Strickholm and Clark, 1977), but for mammalian neurons, information on the quantity of the resting Cl^- permeability or g_{Cl} is scarce. Such information is needed not only to understand recovery of a perturbed $[Cl^-]_i$. The background g_{Cl} is also critically influencing neuronal firing properties, such as action potential frequency adaptation and "after discharge", and the control of cell volume (Berndt et al., 2011). Forsythe and Redman (1988) calculated the approximate resting g_{Cl} in spinal motorneurons to 18% of the total (Na^+, K^+, and Cl^-) conductances, but their estimate depended on several assumptions, including unknown changes in K^+ conductance, and they emphasize the obstacles to estimation introduced by the complex neuronal morphology. In the present work, the latter type of obstacles was avoided by using isolated neuronal cell bodies. Further, the novel method we developed for quantifying g_{Cl} employed a simple expression (Eq. 5), which depended mainly on the testable and verified assumption of constant total conductance in the experimental conditions used. The obtained resting g_{Cl} was relatively low (mean relative g_{Cl} 6% and absolute g_{Cl} 54 pS), with a major (~2/3) contribution by $GABA_A$ receptors, as suggested by the reducing effect of PTX. This corresponds to the conductance of only two open $GABA_A$ receptor channels (with most frequent single-channel conductance of 17 pS; Bormann et al., 1987). Since the presence of δ-subunit-containing $GABA_A$ receptors, which may contribute to tonic currents (Jensen et al., 2013; Wlodarczyk et al., 2013), was suggested above (see Results), it seems likely that such receptors contribute to the $GABA_A$ receptor-mediated fraction of g_{Cl} and $[Cl^-]_i$ recovery. The novel method used here to estimate resting g_{Cl} could easily be applied also to many other preparations. It may be noted that manipulating Cl^- concentrations in the external solution may in many cases provide a useful alternative to loading cells with Cl^-, as done here.

A significant contribution of glycine receptors to the resting g_{Cl} seems unlikely for several reasons. First, the competitive glycine-receptor blocker strychnine did not affect $[Cl^-]_i$ recovery (Fig. 7*A*). Second, in contrast to some $GABA_A$ receptors, glycine receptors do not show any significant degree of spontaneous openings in the absence of ligand (Twyman and Macdonald, 1991; Beato et al., 2002; Bode et al., 2013).

Although ClC-2 channels seem to play a large role for the background conductance in CA1 pyramidal cells (Rinke et al., 2010), we did not find evidence for such channels in MPN neurons. Thus, it is unlikely that they contribute to resting g_{Cl} in these neurons. In cells where ClC-2 channels are present, their contribution to g_{Cl} may be expected to enhance the impact of conductive $[Cl^-]_i$ recovery even beyond that described in the present work. This may be of particular importance if the ClC-2-containing neurons show a limited transporter-dependent recovery capacity, such as indicated by our recordings from hippocampal neurons in the present study.

Role of minis and neurosteroids in Cl^- homeostasis

Spontaneous neurotransmitter release may possibly play a special role in the control of conductive $[Cl^-]_i$ changes. The small postsynaptic currents generated do most often not induce major voltage fluctuations (Miles and Wong, 1986; Sayer et al., 1989; Rotaru et al., 2015). Accordingly, our results showed that, in control conditions, spontaneously released GABA does not significantly affect the recovery of $[Cl^-]_i$ after a high load. However, postsynaptic currents generated by GABA release onto MPN neurons may be prolonged by the action of the endogenous neurosteroid allopregnanolone (Haage

and Johansson, 1999). We here showed that in the presence of a concentration (20 nM) that has been detected *in vivo* when animals are exposed to stress (Purdy et al., 1991), allopregnanolone significantly enhances the speed of $[Cl^-]_i$ recovery. Thus, the neurosteroid has the capacity to control $[Cl^-]_i$ dynamics in a situation when raised $[Cl^-]_i$ seems particularly likely, as a result of stress-induced enhancement of neural activity. Although a stress-induced reduction of inhibition may be important for, e.g., corticotrophin-releasing hormone neurons (Hewitt et al., 2009), it seems likely that other neurons may need a maintained functional inhibition during stress and that allopregnanolone may facilitate this via enhanced conductive $[Cl^-]_i$ recovery. Similarly, neurosteroid-induced enhancement of $[Cl^-]_i$ recovery may likely partly compensate for low levels of KCC2. However, as shown in our computations (Fig. 8*C*), in such situations there will be a trade-off between the rate of recovery and the minimum steady-state $[Cl^-]_i$.

The observed effect of 20 nM allopregnanolone on $[Cl^-]_i$ recovery can be ascribed to the postsynaptic currents (mIPSCs) generated by spontaneously released GABA, since baseline current was not affected. At micromolar concentrations, allopregnanolone directly activates $GABA_A$ receptors as well as potentiates mIPSC frequency and prolongs mIPSC decay in MPN neurons (Haage and Johansson, 1999). In other cells, direct activation of $GABA_A$ receptors may occur at 100 nM allopregnanolone (Shu et al., 2004), a concentration that may be reached during pregnancy (Nguyen et al., 2003), suggesting that steroid modulation of $[Cl^-]_i$ homeostasis via resting g_{Cl} through direct $GABA_A$ receptor activation may be expected under physiologic conditions. Neurosteroid-controlled regulation of Cl^- homeostasis via the channels opened by spontaneously released GABA may possibly provide a novel functional role for spontaneous neurotransmission.

References

Abe Y, Furukawa K, Itoyama Y, Akaike N (1994) Glycine response in acutely dissociated ventromedial hypothalamic neuron of the rat: new approach with gramicidin perforated patch-clamp technique. J Neurophysiol 72:1530–1537. Medline

Ahring PK, Bang LH, Jensen ML, Strøbæk D, Hartiadi LY, Chebib M, Absalom N (2016) A pharmacological assessment of agonists and modulators at $\alpha4\beta2\gamma2$ and $\alpha4\beta2\delta$ $GABA_A$ receptors: the challenge in comparing apples with oranges. Pharmacol Res 111:563–576. CrossRef Medline

Alvarez-Leefmans FJ, Delpire E (2009) Thermodynamics and kinetics of chloride transport in neurons: an outline. In: Physiology and pathology of chloride transporters and channels in the nervous system (Alvarez-Leefmans FJ, Delpire E, eds), pp 81-108. Amsterdam: Academic Press.

Astorga G, Bao J, Marty A, Augustine GJ, Franconville R, Jalil A, Bradley J, Llano I (2015) An excitatory GABA loop operating *in vivo*. Front Cell Neurosci 9:275. CrossRef Medline

Beato M, Groot-Kormelink PJ, Colquhoun D, Sivilotti LG (2002) Openings of the rat recombinant $\alpha1$ homomeric glycine receptor as a function of the number of agonist molecules bound. J Gen Physiol 119:443–466. CrossRef

Belelli D, Harrison NL, Maguire J, Macdonald RL, Walker MC, Cope DW (2009) Extrasynaptic $GABA_A$ receptors: form, pharmacology, and function. J Neurosci 29:12757–12763. CrossRef Medline

Ben-Ari Y (2002) Excitatory actions of GABA during development: the nature of the nurture. Nat Rev Neurosci 3:728–739. CrossRef Medline

Berglund K, Schleich W, Krieger P, Loo LS, Wang D, Cant NB, Feng G, Augustine GJ, Kuner T (2006) Imaging synaptic inhibition in transgenic mice expressing the chloride indicator, Clomeleon. Brain Cell Biol 35:207–228. CrossRef Medline

Berndt N, Hoffman S, Benda J, Holzhütter H-G (2011) The influence of the chloride currents on action potential firing and volume regulation of excitable cells studied by a kinetic model. J Theor Biol 276:42–49. CrossRef

Birnir B, Everitt AB, Lim MS, Gage PW (2000) Spontaneously opening $GABA_A$ channels in CA1 pyramidal neurones of rat hippocampus. J Membr Biol 174:21–29. Medline

Bode A, Wood SE, Mullins JG, Keramidas A, Cushion TD, Thomas RH, Pickrell WO, Drew CJ, Masri A, Jones EA, Vassallo G, Born AP, Alehan F, Aharoni S, Bannasch G, Bartsch M, Kara B, Krause A, Karam EG, Matta S, et al. (2013) New hyperekplexia mutations provide insight into glycine receptor assembly, trafficking, and activation mechanisms. J Biol Chem 288:33745–33759. CrossRef Medline

Bormann J, Hamill OP, Sakmann B (1987) Mechanism of anion permeation through channels gated by glycine and γ-aminobutyric acid in mouse cultured spinal neurones. J Physiol 385:243–286. Medline

Boulenguez P, Liabeuf S, Bos R, Bras H, Jean-Xavier C, Brocard C, Stil A, Darbon P, Cattaert D, Delpire E, Marsala M, Vinay L (2010) Down-regulation of the potassium-chloride cotransporter KCC2 contributes to spasticity after spinal cord injury. Nat Med 16:302–307. CrossRef Medline

Chabwine JN, Van Damme P, Eggermont J, De Smedt H, Missiaen L, Van Den Bosch L, Parys JB, Robberecht W, Callewaert G (2004) Long-lasting changes in GABA responsiveness in cultured neurons. Neurosci Lett 365:69–72. CrossRef Medline

Chavas J, Marty A (2003) Coexistence of excitatory and inhibitory GABA synapses in the cerebellar interneuron network. J Neurosci 23:2019–2031. Medline

Coull JAM, Boudreau D, Bachand K, Prescott SA, Nault F, Sík A, D, Koninck P, D, Koninck Y (2003) Trans-synaptic shift in anion gradient in spinal lamina I neurons as a mechanism of neuropathic pain. Nature 424:938–942. CrossRef

Deisz RA, Lehmann T-N, Horn P, Dehnicke C, Nitsch R (2011) Components of neuronal chloride transport in rat and human neocortex. J Physiol 589:1317–1347. CrossRef Medline

Doyon N, Prescott SA, Castonguay A, Godin AG, Kröger H, De Koninck Y (2011) Efficacy of synaptic inhibition depends on multiple, dynamically interacting mechanisms implicated in chloride homeostasis. PLoS Comput Biol 7:e1002149. CrossRef Medline

Doyon N, Prescott SA, De Koninck Y (2016a) Mild KCC2 Hypofunction causes inconspicuous chloride dysregulation that degrades neural coding. Front Cell Neurosci 9:516. CrossRef

Doyon N, Vinay L, Prescott SA, De Koninck Y (2016b) Chloride regulation: a dynamic equilibrium crucial for synaptic inhibition. Neuron 89:1157–1172. CrossRef Medline

Druzin M, Johansson S (2016) 2-Aminoethyl diphenylborinate blocks $GABA_A$-receptor-mediated currents in rat medial preoptic neurons. Opera Med Physiol 2:63–68.

Etter A, Cully DF, Liu KK, Reiss B, Vassilatis DK, Schaeffer JM, Arena JP (1999) Picrotoxin blockade of invertebrate glutamate-gated chloride channels: subunit dependence and evidence for binding within the pore. J Neurochem 72:318–326. CrossRef

Forsythe ID, Redman SJ (1988) The dependence of motoneurone membrane potential on extracellular ion concentrations studied in isolated rat spinal cord. J Physiol 404:83–99. Medline

Földy C, Lee S-H, Morgan RJ, Soltesz I (2010) Regulation of fast-spiking basket cell synapses by the chloride channel ClC-2. Nat Neurosci 13:1047–1049. CrossRef Medline

Friedel P, Kahle KT, Zhang J, Hertz N, Pisella LI, Buhler E, Schaller F, Duan JJ, Khanna AR, Bishop PN, Shokat KM, Medina I (2015) WNK1-regulated inhibitory phosphorylation of the KCC2 cotrans-

porter maintains the depolarizing action of GABA in immature neurons. Sci Signal 8:ra65. CrossRef
Goldman DE (1943) Potential, impedance, and rectification in membranes. J Gen Physiol 27:37–60. Medline
Haage D, Druzin M, Johansson S (2002) Allopregnanolone modulates spontaneous GABA release via presynaptic Cl^- permeability in rat preoptic nerve terminals. Brain Res 958:405–413. Medline
Haage D, Johansson S (1999) Neurosteroid modulation of synaptic and GABA-evoked currents in neurons from the rat medial preoptic nucleus. J Neurophysiol 82:143–151. Medline
Haage D, Karlsson U, Johansson S (1998) Heterogeneous presynaptic Ca^{2+} channel types triggering GABA release onto medial preoptic neurons from rat. J Physiol 507:77–91. CrossRef
Hamann M, Desarmenien M, Desaulles E, Bader MF, Feltz P (1988) Quantitative evaluation of the properties of a pyridazinyl GABA derivative (SR 95531) as a $GABA_A$ competitive antagonist. An electrophysiological approach. Brain Res 442:287–296. Medline
Heaulme M, Chambon JP, Leyris R, Molimard JC, Wermuth CG, Biziere K (1986) Biochemical characterization of the interaction of three pyridazinyl-GABA derivatives with the $GABA_A$ receptor site. Brain Res 384:224–231. Medline
Hewitt SA, Wamsteeker JI, Kurz EU, Bains JS (2009) Altered chloride homeostasis removes synaptic inhibitory constraint of the stress axis. Nat Neurosci 12:438–443. CrossRef Medline
Hodgkin AL, Katz B (1949) The effect of sodium ions on the electrical activity of giant axon of the squid. J Physiol 108:37–77. Medline
Huberfeld G, Wittner L, Clemenceau S, Baulac M, Kaila K, Miles R, Rivera C (2007) Perturbed chloride homeostasis and GABAergic signaling in human temporal lobe epilepsy. J Neurosci 27:9866–9873. CrossRef Medline
Jaenisch N, Witte OW, Frahm C (2010) Downregulation of potassium chloride cotransporter KCC2 after transient focal cerebral ischemia. Stroke 41:e151–e159. CrossRef
Jensen ML, Wafford KA, Brown AR, Belelli D, Lambert JJ, Mirze NR (2013) A study of subunit selectivity, mechanism and site of action of the delta selective compound 2 (DS2) at human recombinant and rodent native $GABA_A$ receptors. Br J Pharmacol 168:1118–1132. CrossRef
Johansson S, Yelhekar TD, Druzin M (2016) Commentary: chloride regulation: a dynamic equilibration crucial for synaptic inhibition. Front Cell Neurosci 10:182. CrossRef
Kaila K, Price TJ, Payne JA, Puskarjov M, Voipio J (2014) Cation-chloride cotransporters in neuronal development, plasticity and disease. Nat Rev Neurosci 15:637–654. CrossRef Medline
Karlsson U, Druzin M, Johansson S (2011) Cl^- concentration changes and desensitization of $GABA_A$ and glycine receptors. J Gen Physiol 138:609–626. CrossRef Medline
Karlsson U, Sundgren AK, Näsström J, Johansson S (1997) Glutamate-evoked currents in acutely dissociated neurons from the rat medial preoptic nucleus. Brain Res 759:270–276. Medline
Khalilov I, Holmes GL, Ben-Ari Y (2003) *In vitro* formation of a secondary epileptogenic mirror focus by interhippocampal propagation of seizures. Nat Neurosci 6:1079–1085. CrossRef Medline
Koester J, Siegelbaum SA (2013) Membrane potential and the passive electrical properties of the neuron. In: Principles of neural science, Ed 5 (Kandel ER, Schwartz JH, Jessell TM, Siegelbaum SA, Hudspeth AJ, eds), pp 126–147. New York: Mc Graw Hill.
Kyrozis A, Reichling DB (1995) Perforated-patch recording with gramicidin avoids artifactual changes in intracellular chloride concentration. J Neurosci Methods 57:27–35. Medline
Lee HHC, Deeb TZ, Walker JA, Davies PA, Moss SJ (2011) NMDA receptor activity downregulates KCC2 resulting in depolarizing $GABA_A$ receptor-mediated currents. Nat Neurosci 14:736–743. CrossRef
Merner ND, Chandler MR, Bourassa C, Liang B, Khanna AR, Dion P, Rouleau GA, Kahle KT (2015) Regulatory domain or CpG site variation in SLC12A5, encoding the chloride transporter KCC2, in human autism and schizophrenia. Front Cell Neurosci 9:386. CrossRef Medline
Miles R, Wong RK (1986) Excitatory synaptic interactions between CA3 neurones in the guinea-pig hippocampus. J Physiol 373:397–418. Medline
Müller M (2000) Effects of chloride transport inhibition and chloride substitution on neuron function and on hypoxic spreading-depression-like depolarization in rat hippocampal slices. Neuroscience 97:33–45. Medline
Nguyen PN, Billiards SS, Walker DW, Hirst JJ (2003) Changes in 5α-pregnane steroids and neurosteroidogenic enzyme expression in the perinatal sheep. Pediatr Res 53:956–964. CrossRef Medline
Pellegrino C, Gubkina O, Schaefer M, Becq H, Ludwig A, Mukhtarov M, Chudotvorova I, Corby S, Salyha Y, Salozhin S, Bregestovski P, Medina I (2011) Knocking down of the KCC2 in rat hippocampal neurons increases intracellular chloride concentration and compromises neuronal survival. J Physiol 589:2475–2496. CrossRef Medline
Purdy RH, Morrow AL, Moore PH, Paul SM (1991) Stress-induced elevations of γ-aminobutyric acid type A receptor-active steroids in the rat brain. Proc Natl Acad Sci USA 88:4553–4557. Medline
Pusch M, Neher E (1988) Rates of diffusional exchange between small cells and a measuring patch pipette. Pflügers Arch Eur J Physiol 411:204–211. CrossRef
Rae J, Cooper K, Gates P, Watsky M (1991) Low access resistance perforated patch recordings using amphotericin B. J Neurosci Methods 37:15–26. Medline
Rinke I (2010) Chloride regulatory mechanisms and their influence on neuronal excitability. Doctoral thesis from der Ludwig-Maximilians-Universität München. Available at https://edoc.ub.uni-muenchen.de/12513/1/Rinke_Ilka.pdf.
Rinke I, Artmann J, Stein V (2010) ClC-2 voltage-gated channels constitute part of the background conductance and assist chloride extrusion. J Neurosci 30:4776–4786. CrossRef Medline
Rotaru DC, Olezene C, Miyamae T, Povysheva NV, Zaitsev AV, Lewis DA, Gonzalez-Burgos G (2015) Functional properties of GABA synaptic inputs onto GABA neurons in monkey prefrontal cortex. J Neurophysiol 113:1850–1861. CrossRef Medline
Russell JM, Brown AM (1972) Active transport of chloride by the giant neuron of the *Aplysia* abdominal ganglion. J Gen Physiol 60:499–518. Medline
Sacchi O, Rossi ML, Canella R, Fesce R (1999) Participation of a chloride conductance in the subthreshold behavior of the rat sympathetic neuron. J Neurophysiol 82:1662–1675. CrossRef
Sayer RJ, Redman SJ, Andersen P (1989) Amplitude fluctuations in small EPSPs recorded from CA1 pyramidal cells in the guinea pig hippocampal slice. J Neurosci 9:840–850. Medline
Semyanov A, Walker MC, Kullmann DM, Silver RA (2004) Tonically active $GABA_A$ receptors: modulating gain and maintaining the tone. Trends Neurosci 27:262–269. CrossRef Medline
Shu H-J, Eisenman LN, Jinadasa D, Covey DF, Zorumski CF, Mennerick S (2004) Slow actions of neuroactive steroids at $GABA_A$ receptors. J Neurosci 24:6667–6675. CrossRef Medline
Smith RL, Clayton GH, Wilcox CL, Escudero KW, Staley KJ (1995) Differential expression of an inwardly rectifying chloride conductance in rat brain neurons: a potential mechanism for cell-specific modulation of postsynaptic inhibition. J Neurosci 15:4057–4067. Medline
Staley KJ, Proctor WR (1999) Modulation of mammalian dendritic $GABA_A$ receptor function by the kinetics of Cl^- and HCO_3^- transport. J Physiol 519:693–712. CrossRef
Stell BM, Brickley SG, Tang CY, Farrant M, Mody I (2003) Neuroactive steroids reduce neuronal excitability by selectively enhancing tonic inhibition mediated by δ subunit-containing $GABA_A$ receptors. Proc Natl Acad Sci USA 100:14439–14444.
Stölting G, Fischer M, Fahlke C (2014) CLC channel function and dysfunction in health and disease. Front Physiol 5:378. CrossRef Medline
Strickholm A, Clark HR (1977) Ionic permeability of K, Na, and Cl in crayfish nerve. Regulation by membrane fixed charges and pH. Biophys J 19:29–48. CrossRef Medline

Takeuchi A, Takeuchi N (1969) A study of the action of picrotoxin on the inhibitory neuromuscular junction of the crayfish. J Physiol 205:377–391. Medline

Thompson SM, Deisz RA, Prince DA (1988) Relative contributions of passive equilibrium and active transport to the distribution of chloride in mammalian cortical neurons. J Neurophysiol 60:105–124. Medline

Twyman RE, Macdonald RL (1991) Kinetic properties of the glycine receptor main- and sub-conductance states of mouse spinal cord neurones in culture. J Physiol 435:303–331. Medline

Tyzio R, Nardou R, Ferrari DC, Tsintsadze T, Shahrokhi A, Eftekhari S, Khalilov I, Tsintsadze V, Brouchoud C, Chazal G, Lemonnier E, Lozovaya N, Burnashev N, Ben-Ari Y (2014) Oxytocin-mediated GABA inhibition during delivery attenuates autism pathogenesis in rodent offspring. Science 343:675–679. CrossRef Medline

Wafford KA, van Niel MB, Ma QP, Horridge E, Herd MB, Peden DR, Belelli D, Lambert JJ (2009) Novel compounds selectively enhance δ subunit containing $GABA_A$ receptors and increase tonic currents in thalamus. Neuropharmacology 56:182–189. CrossRef

Wagner S, Sagiv N, Yarom Y (2001) GABA-induced current and circadian regulation of chloride in neurones of the rat suprachiasmatic nucleus. J Physiol 537:853–869. Medline

Wang DD, Krueger DD, Bordey A (2003) GABA depolarizes neuronal progenitors of the postnatal subventricular zone via $GABA_A$ receptor activation. J Physiol 550:785–800. CrossRef Medline

Wlodarczyk AI, Sylantyev S, Herd MB, Kersanté F, Lambert JJ, Rusakov DA, Linthorst ACE, Semyanov A, Belelli D, Pavlov I, Walker MC (2013) GABA-independent $GABA_A$ receptor openings maintain tonic currents. J Neurosci 33:3905–3914. CrossRef

Yelhekar TD, Druzin M, Karlsson U, Blomqvist E, Johansson S (2016) How to properly measure a current-voltage relation?—Interpolation vs. ramp methods applied to studies of $GABA_A$ receptors. Front Cell Neurosci 10:10. CrossRef